Radisav, Vidic 5/20/25

VOLS. 65–66
Completing vols. 65–66

JUNE 2000

ISSN 0378-3820

Fuel Processing Technology

Special Issue

Air Quality:
Mercury, Trace Elements
and Particulate Matter

ELSEVIER

www.elsevier.com/locate/fuproc

Radisav, Vidic 5/20/25

FUEL PROCESSING TECHNOLOGY

An international journal devoted to all aspects of processing and beneficiation of coal, petroleum, oil shale, tar sands and peat

Volumes 65–66 (2000)

ELSEVIER Fuel Processing Technology 65–66 (2000) 289–310

FUEL
PROCESSING
TECHNOLOGY

www.elsevier.com/locate/fuproc

Mercury transformations in coal combustion flue gas

Kevin C. Galbreath *, Christopher J. Zygarlicke

Energy and Environmental Research Center, University of North Dakota, Grand Forks, ND 58202-9018, USA

Received 12 February 1999; accepted 12 May 1999

Abstract

Mercury chlorination [i.e., formation of $\mathrm{HgCl_2(g)}$] is generally assumed to be the dominant mercury-transformation mechanism in coal combustion flue gas. Other potential mechanisms involve mercury interactions with ash particle surfaces where reactive chemical species, oxidation catalysts, and active sorption sites are available to transform $\mathrm{Hg^0(g)}$ to $\mathrm{Hg^{2+}X(g)}$ (e.g., where X is $\mathrm{Cl_2}$ or O) as well as $\mathrm{Hg^0(g)}$ and $\mathrm{HgCl_2(g)}$ to particulate mercury, Hg(p). Results from an investigation of $\mathrm{Hg^0(g)–O_2(g)–HCl(g)}$ and $\mathrm{Hg^{0,2+}(g)–HCl(g)–CaO(s)}$-fly ash interactions in a 42-MJ/h combustion system are consistent with the following mechanisms: mercury chlorination, catalysis of mercury oxidation by $\mathrm{Al_2O_3(s)}$ and/or $\mathrm{TiO_2(s)}$, and mercury sorption on a calcium-rich (25.0 wt.% CaO) subbituminous coal fly ash. Additions of 50 and 100 ppmv of HCl(g) and ≈ 12.6 wt.% of CaO(s) to the subbituminous coal combustion environment inhibited Hg(p) formation, primarily via a change in ash surface chemistry and a decrease in particle surface area, respectively. © 2000 Elsevier Science B.V. All rights reserved.

Keywords: Mercury; Speciation; Transformations; Air toxics; Hazardous air pollutants; Coal; Combustion

1. Introduction

According to the Mercury Study Report to Congress, coal combustion is the primary source of anthropogenic mercury emissions in the United States, accounting for 72 of the 158 tons/yr of total point-source mercury emissions [1]. Knowledge of mercury physical and chemical transformations in coal combustion flue gas is imperative for understanding the transport and fate of mercury released into air pollution control

---

* Corresponding author. Tel.: +1-701-777-5127; fax: +1-701-777-5181; e-mail: kgalbreath@eerc.und.nodak.edu

PII: S0378-3820(99)00102-2

systems and the atmosphere. The current knowledge of mercury transformations in coal combustion flue gas is based largely on thermodynamic modeling and experimental investigations of mercury reactions in simulated flue gases and, to a limited extent, on the interpretations of field test data [2,3]. Mercury exists primarily as gaseous (g) elemental mercury, $Hg^0(g)$, and as gaseous or solid (s) inorganic mercuric compounds, $Hg^{2+}X$ [e.g., where X is $Cl_2(g)$, $SO_4(s)$, O(s,g), S(s)], in coal combustion flue gas. Mercury emissions from coal-fired boilers can be empirically classified, based on the capabilities of currently available analytical methods for determining mercury speciation, into three main forms: $Hg^0(g)$, $Hg^{2+}X(g)$, and particulate mercury, Hg(p). Mercury concentrations in coal combustion flue gas generally range from 5 to 10 $\mu g/m^3$, with a large range in the relative proportions of $Hg^0(g)$, $Hg^{2+}X(g)$, and Hg(p).

During combustion, $Hg^0(g)$ is liberated from coal. A significant fraction of the $Hg^0(g)$, however, is generally transformed to $Hg^{2+}X(g)$ and Hg(p) in the postcombustion environment of a coal-fired boiler. $Hg^0(g)$ is the most abundant and persistent (residence time of 0.5 to 2 years) form of mercury in the atmosphere [4–7]. Relative to $Hg^0(g)$, $Hg^{2+}X(g)$ and Hg(p) are more effectively captured in conventional pollution control systems (wet scrubbers and fabric filters) and are more apt to deposit locally or regionally [2,6,8,9]. Mercury emission control efficiencies and transport/deposition models for coal-fired boilers can be improved by identifying the fundamental mechanisms involved in mercury–flue gas interactions that transform $Hg^0(g)$ to $Hg^{2+}X(g)$ and Hg(p).

Mercury interactions with inorganic and carbonaceous ash particles entrained in coal combustion flue gas (i.e., fly ash), especially at the gas–particulate surface interface, are important to consider in understanding mercury transformations. Reactive chemical species and oxidation catalysts on fly ash particles can convert $Hg^0(g)$ to $Hg^{2+}X(g)$. Fly ash particle surfaces may also host active sites for mercury adsorption. Measurements by Otani et al. [10], Schager et al. [11], Hall et al. [12], and Carey et al. [13] indicate that some fly ashes actually adsorb mercury at rates greater than various sorbents, including activated carbon. Brown [14] reviewed mercury speciation analysis results and identified several coals that produce significant concentrations of $Hg^{2+}X(g)$ and/or Hg(p) in the postcombustion environment of pilot- and full-scale utility boilers. Apparently the flue gases and/or fly ashes produced from certain coals possess intrinsic properties that promote mercury oxidation and/or mercury–ash sorption. Mercury sorption by fly ash can occur via physical adsorption, chemisorption, chemical reaction, or a combination of these processes. Although it is well established that fly ash particles capture mercury species, the nature of mercury–fly ash interactions is not well understood.

In this paper, information that pertains primarily to mercury–fly ash interactions is reviewed to identify the fundamental mechanisms involved in mercury combustion transformations. This review supplements those by Galbreath and Zygarlicke [2] and Laudal et al. [Section 2 in Ref. [3]] that focus on potential interactions between mercury species and gaseous flue gas components. Results from an on-going investigation of mercury transformations using a laboratory-scale (42-MJ/h) combustion system are also presented. Preliminary observations and conclusions from this investigation corroborate the importance of particulate–surface interactions in controlling high-temperature (≥ 250°C) mercury transformations.

2. Overview of mercury coal combustion transformations

Plausible physical and chemical transformations that mercury undergoes during coal combustion and subsequently in the resulting flue gas are summarized in Fig. 1. Mercury is associated primarily with the inorganic mineral components of coal, although an association with the organic maceral components of coal as organomercuric compounds has been suggested [15–17]. Mercury is classified geochemically as a chalcophile element [18]. Accordingly, pyrite (FeS_2) and cinnabar (HgS) are the dominant mineral hosts for mercury in coal. As the mineral and possibly organomercuric hosts of mercury decompose during combustion (> 1400°C), mercury is liberated as $Hg^0(g)$ (boiling point of 357°C at 1 atm, vapor pressure of 0.180 Pa at 20°C). In contrast to the nonvolatile and semivolatile trace elements in coal, the mode of occurrence of mercury (i.e., mineral or maceral association) does not affect this initial combustion transformation mechanism.

In the chemically complex postcombustion environment and with decreasing temperature, $Hg^0(g)$ may remain as a monatomic species or react to form inorganic mercurous (Hg_2^{2+}) and Hg^{2+} compounds. The principal oxidized forms of mercury in coal combustion flue gas are assumed to be Hg^{2+} compounds because of the instability of Hg_2^{2+} compounds at low concentrations (i.e., in dilute solutions) [19]. Mercury chlorination, the reaction of $Hg^0(g)$ with HCl(g) or $Cl_2(g)$ to form $HgCl_2(g)$, is generally

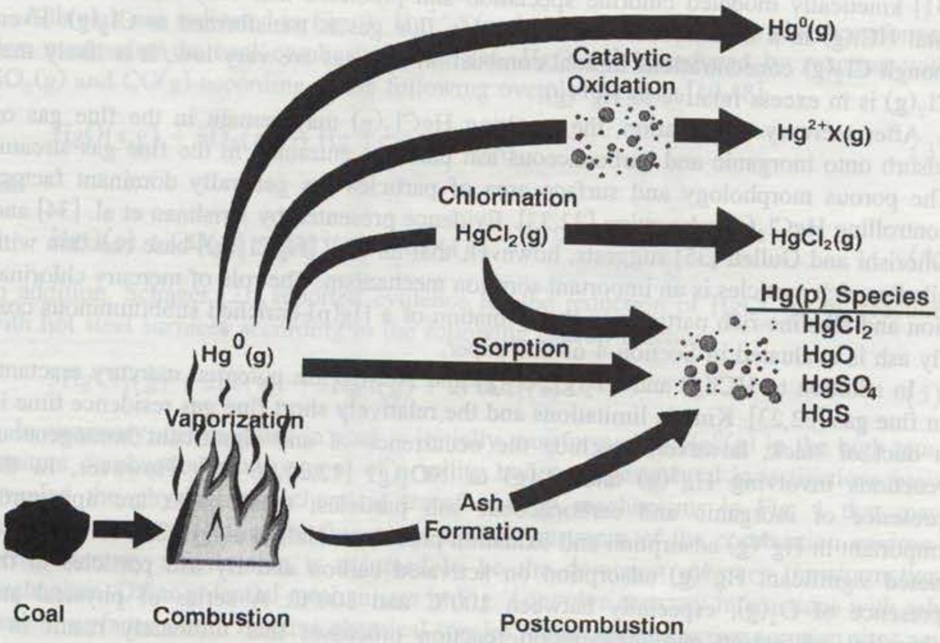

Fig. 1. Potential mercury transformations during coal combustion and subsequently in the resulting flue gas.

e. The current knowledge of mercury transformations in coal
sed largely on thermodynamic modeling and experimental
eactions in simulated flue gases and, to a limited extent, on
l test data [2,3]. Mercury exists primarily as gaseous (g)
, and as gaseous or solid (s) inorganic mercuric compounds,
Cl_2(g), SO_4(s), O(s,g), S(s)], in coal combustion flue gas.
oal-fired boilers can be empirically classified, based on the
vailable analytical methods for determining mercury specia-
ms: Hg^0(g), $Hg^{2+}X$(g), and particulate mercury, Hg(p).
coal combustion flue gas generally range from 5 to 10
in the relative proportions of Hg^0(g), $Hg^{2+}X$(g), and Hg(p).
^{0}(g) is liberated from coal. A significant fraction of the
lly transformed to $Hg^{2+}X$(g) and Hg(p) in the postcombus-
l-fired boiler. Hg^0(g) is the most abundant and persistent
years) form of mercury in the atmosphere [4–7]. Relative to
(p) are more effectively captured in conventional pollution
ers and fabric filters) and are more apt to deposit locally or
ry emission control efficiencies and transport/deposition
s can be improved by identifying the fundamental mecha-
flue gas interactions that transform Hg^0(g) to $Hg^{2+}X$(g) and

inorganic and carbonaceous ash particles entrained in coal
ash), especially at the gas–particulate surface interface, are
nderstanding mercury transformations. Reactive chemical
ts on fly ash particles can convert Hg^0(g) to $Hg^{2+}X$(g). Fly
o host active sites for mercury adsorption. Measurements by
al. [11], Hall et al. [12], and Carey et al. [13] indicate that
rb mercury at rates greater than various sorbents, including
reviewed mercury speciation analysis results and identified
gnificant concentrations of $Hg^{2+}X$(g) and/or Hg(p) in the
of pilot- and full-scale utility boilers. Apparently the flue
duced from certain coals possess intrinsic properties that
and/or mercury–ash sorption. Mercury sorption by fly ash
tion, chemisorption, chemical reaction, or a combination of
is well established that fly ash particles capture mercury
y–fly ash interactions is not well understood.
that pertains primarily to mercury–fly ash interactions is
ndamental mechanisms involved in mercury combustion
supplements those by Galbreath and Zygarlicke [2] and
f. [3]] that focus on potential interactions between mercury
s components. Results from an on-going investigation of
a laboratory-scale (42-MJ/h) combustion system are also
ations and conclusions from this investigation corroborate
–surface interactions in controlling high-temperature (≥
ns.

2. Overview of mercury coal combustion transformations

Plausible physical and chemical transformations that mercury undergoes during coal combustion and subsequently in the resulting flue gas are summarized in Fig. 1. Mercury is associated primarily with the inorganic mineral components of coal, although an association with the organic maceral components of coal as organomercuric compounds has been suggested [15–17]. Mercury is classified geochemically as a chalcophile element [18]. Accordingly, pyrite (FeS_2) and cinnabar (HgS) are the dominant mineral hosts for mercury in coal. As the mineral and possibly organomercuric hosts of mercury decompose during combustion (> 1400°C), mercury is liberated as Hg^0(g) (boiling point of 357°C at 1 atm, vapor pressure of 0.180 Pa at 20°C). In contrast to the nonvolatile and semivolatile trace elements in coal, the mode of occurrence of mercury (i.e., mineral or maceral association) does not affect this initial combustion transformation mechanism.

In the chemically complex postcombustion environment and with decreasing temperature, Hg^0(g) may remain as a monatomic species or react to form inorganic mercurous (Hg_2^{2+}) and Hg^{2+} compounds. The principal oxidized forms of mercury in coal combustion flue gas are assumed to be Hg^{2+} compounds because of the instability of Hg_2^{2+} compounds at low concentrations (i.e., in dilute solutions) [19]. Mercury chlorination, the reaction of Hg^0(g) with HCl(g) or Cl_2(g) to form $HgCl_2$(g), is generally

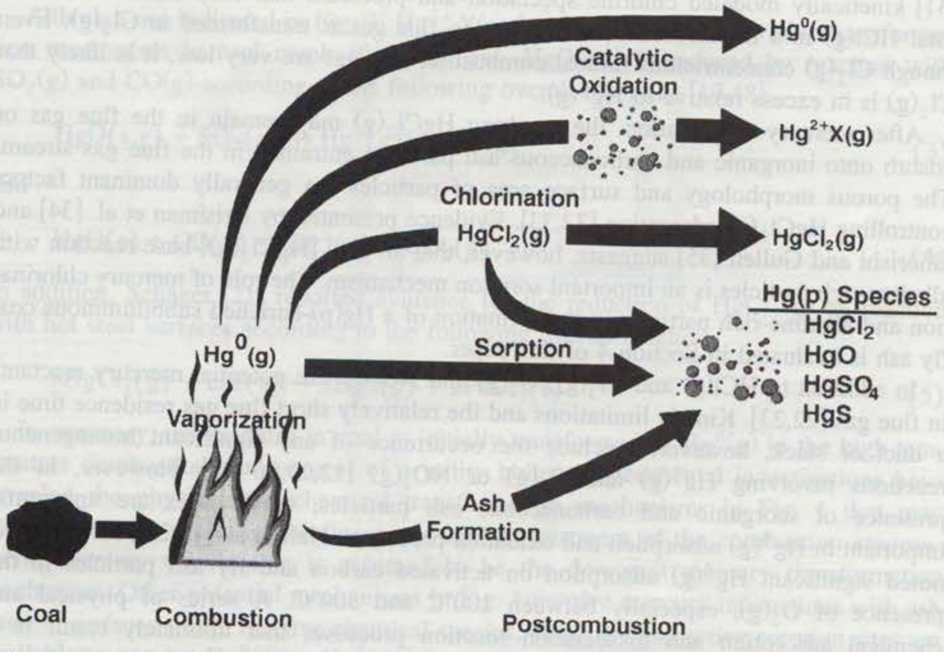

Fig. 1. Potential mercury transformations during coal combustion and subsequently in the resulting flue gas.

considered to be the dominant mercury transformation mechanism in coal combustion flue gas, even though $HgCl_2(g)$ has never been directly measured. HCl(g) concentrations in coal combustion flue gas range from about 25 to 150 mg/m^3 [20]. Theoretical and experimental investigations indicate that although HCl(g) will react with $Hg^0(g)$, $Cl_2(g)$ is a much more active mercury-chlorinating agent [21–25]. Consequently, chlorine speciation is an important factor to consider in understanding flue gas mercury transformations. Chlorine is evolved from coal during combustion primarily as HCl(g) [26]. In the postcombustion environment, $Cl_2(g)$ is presumably formed according to the following Deacon process reaction [27]:

$$2HCl(g) + 1/2O_2(g) \overset{\text{catalyst}}{\rightarrow} Cl_2(g) + H_2O(g) \tag{1}$$

Although the Deacon reaction is thermodynamically favorable at relatively low temperatures (430–475°C), it proceeds only in the presence of metal catalyst species [28]. Experimental investigations indicate that the presence of $SO_2(g)$ in combustion flue gas can inhibit the formation of chlorinated compounds by depleting $Cl_2(g)$ concentrations according to the following net overall reaction:

$$Cl_2(g) + SO_2(g) + H_2O(g) \rightleftarrows 2HCl(g) + SO_3(g) \tag{2}$$

or by reducing the catalytic activity of fly ash [29,30]. Consequently, a high sulfur–chlorine ratio inhibits the formation of $Cl_2(g)$ and subsequently of $HgCl_2(g)$. Realizing that the formation of $Cl_2(g)$ is not governed by thermochemical equilibrium, Senior et al. [31] kinetically modeled chlorine speciation and predicted that only about 1% of the total HCl(g) in a bituminous coal combustion flue gas is transformed to $Cl_2(g)$. Even though $Cl_2(g)$ concentrations in coal combustion flue gas are very low, it is likely that $Cl_2(g)$ is in excess relative to $Hg^0(g)$.

After mercury chlorination, the resulting $HgCl_2(g)$ may remain in the flue gas or adsorb onto inorganic and carbonaceous ash particles entrained in the flue gas stream. The porous morphology and surface area of particles are generally dominant factors controlling $HgCl_2(g)$ adsorption [32,33]. Evidence presented by Krishnan et al. [34] and Ghorishi and Gullett [35] suggests, however, that an acid [$HgCl_2(g)$]-base reaction with alkaline-rich particles is an important sorption mechanism. The role of mercury chlorination and alkaline-rich particles in the formation of a Hg(p)-enriched subbituminous coal fly ash is evaluated in Section 4 of this paper.

In addition to HCl(g) and $Cl_2(g)$, $O_2(g)$ and $NO_2(g)$ are potential mercury reactants in flue gas [22,23]. Kinetic limitations and the relatively short flue gas residence time in a duct or stack, however, preclude the occurrence of any significant homogeneous reactions involving $Hg^0(g)$ and $O_2(g)$ or $NO_2(g)$ [12,25,36–38]. However, in the presence of inorganic and carbonaceous ash particles, these gases are apparently important in $Hg^0(g)$ adsorption and oxidation processes. Hall et al. [12,23], for example, noted significant $Hg^0(g)$ adsorption on activated carbon and fly ash particles in the presence of $O_2(g)$, especially between 100°C and 300°C. A series of physical and chemical adsorption and dissociation reaction processes that ultimately result in a reaction between $Hg^0(g)$ and atomic oxygen to form HgO(s) on particle surfaces was proposed to explain mercury adsorption. During an investigation of the effects of flue gas components (O_2, CO_2, H_2O, N_2, SO_2, HCl, NO, NO_2, HF, Cl_2) on Hg^0(g)–fly ash and Hg^0(g)–carbon sorbent interactions in heated (< 200°C) simulated flue gases, Laudal et al. [38] and Miller et al. [39] found that the presence of NO_2(g) inhibits Hg^0(g) adsorption but promotes the formation of $Hg^{2+}X$(g). This effect was noted for NO_2(g) concentrations as low as 20 ppmv [39]. Carey et al. [13] also showed that in a heated (≤ 370°C) simulated flue gas, the presence of fly ash and certain ash components (iron and alumina compounds) promotes the conversion of Hg^0(g) to $Hg^{2+}X$(g). The presence of oxygenated and nitrogenated species and oxidation catalysts on fly ash particle surfaces appears to be an important factor controlling the transformation of Hg^0(g) to Hg(p) and $Hg^{2+}X$(g).

Sulfur-rich ash particles entrained in coal combustion flue gas are potential reactants and sorbents for Hg^0(g). During combustion, sulfur is released from coal as SO_2(g). A fraction of the SO_2(g), generally 1–3% [40], is oxidized to SO_3(g). The formation of SO_3(g) is catalyzed by transition metal oxide (e.g., Fe_2O_3) components of submicrometer ash but is neutralized by alkali and alkaline-earth metals in ash [41]. SO_3(g) reacts with H_2O(g) in flue gas to form H_2SO_4(g). At temperatures below the sulfuric acid dew point, H_2SO_4(l) condenses on ash particle surfaces and mercury species may absorb in H_2SO_4(l) [42]. Mercury sulfation products resulting from HgO(s)–SO_2(g)–O_2(g)–H_2O(l) interactions have been identified by Shashkov et al. [43] and Zacharewski et al. [44]. In addition to H_2SO_4(l) condensation on particle surfaces, the chemisorption of sulfur compounds onto particle surfaces may create active mercury sorption sites. Indeed, chemisorption is used to create sulfur-impregnated sorbents for removing mercury from gas streams as adsorbed HgS [45–47].

Although not indicated in Fig. 1, $Hg^{2+}X$(s,g) reduction may be a viable transformation mechanism in coal combustion flue gas. HgO(s,g) is reduced by reaction with SO_2(g) and CO(g) according to the following overall reactions [19,48]:

$$\mathrm{HgO(s,g)} + \mathrm{SO_2(g)} \rightarrow \mathrm{Hg^0(g)} + \mathrm{SO_3(g)} \tag{3}$$

and

$$\mathrm{HgO(s)} + \mathrm{CO(g)} \rightarrow \mathrm{Hg^0(g)} + \mathrm{CO_2(g)}. \tag{4}$$

In addition, Schager [21] reported evidence for the reduction of $HgCl_2$(g) by reaction with hot steel surfaces according to the following overall reaction:

$$3\mathrm{HgCl_2(g)} + 2\mathrm{Fe(s)} \rightarrow 3\mathrm{Hg^0(g)} + 2\mathrm{FeCl_3(s)} \tag{5}$$

In summary, the mercury in coal is initially transformed to Hg^0(g) in the high-temperature combustion environment of a utility boiler. Experimental investigations have revealed the physical and chemical transformation mechanisms in Fig. 1 that may control mercury speciation as flue gases cool downstream of the combustion environment. Mercury chlorination is assumed to be the dominant mercury transformation mechanism. Other potential mechanisms in Fig. 1 involve mercury interactions with ash particle surfaces where reactive chemical species, catalysts, and active sorption sites are available to convert Hg^0(g) to $Hg^{2+}X$(g) as well as Hg^0(g) and $HgCl_2$(g) to Hg(p).

3. Mercury–oxygen–chlorine interactions in a laboratory combustion system

Tests involving the injection of 10 μg/m^3 $Hg^0(g)$ and 100 ppmv HCl(g) into a simple gas mixture of 8.5 mol% O_2 and ≈ 91.5 mol% N_2 were performed using a 42-MJ/h combustion system. Although these tests were originally intended for evaluating quality control [$Hg^0(g)$ and HCl(g) spike recoveries], test results revealed significant Hg^0–O_2–Cl interactions with insulating components of the combustor. These interactions may be relevant to mercury–fly ash interactions because the chemical and mineralogical compositions of the insulation are similar to the composition of coal fly ash.

3.1. Experimental

A schematic of the 42-MJ/h combustion system is presented in Fig. 2. Internal components of the system are composed primarily of Alumina 998 ceramic and Narcast 60 refractory materials to minimize contamination from metal surfaces. Sampling and HCl(g) and $Hg^0(g)$ injection locations, as well as gas temperatures at these locations, are indicated in Fig. 2. A cylinder of working-standard-grade HCl(g) (10,290 ± 510 ppmv HCl in N_2) and a permeation device (VICI Metronics) were used as sources of HCl(g) and $Hg^0(g)$, respectively. The concentration of HCl(g) was controlled using a calibrated

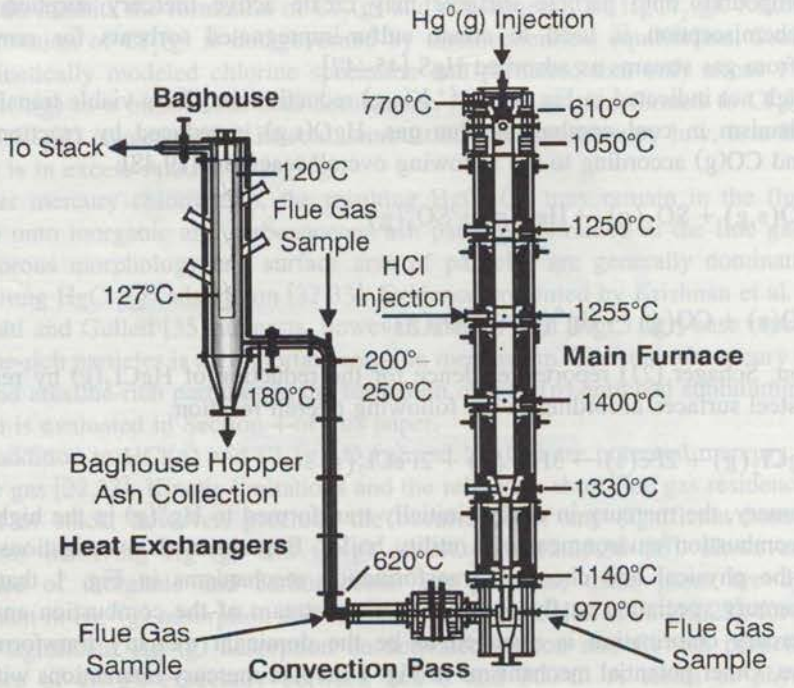

Fig. 2. Schematic of the 42-MJ/h downfired combustor showing the sampling and spiking locations as well as flue gas temperatures resulting from the heating of a gas mixture (8.5% O_2, 91.5% N_2).

flowmeter. $Hg^0(g)$ concentration was controlled by varying the temperature of the permeation tube and the gas flow rate of a N_2 carrier gas. An on-line mercury analyzer (Semtech Hg 2000 or P.S. Analytical, Sir Galahad) was used to verify $Hg^0(g)$ spike concentration. Residence time of injected $Hg^0(g)$ in the combustor was approximately 2.5 s. Concentrations of major flue gas components [e.g., $O_2(g)$ and $NO_x(g)$] were measured in the combustor using on-line analyzers (Beckman Instruments). The system was maintained at the temperatures indicated in Fig. 2 overnight prior to each test to minimize cross-contamination of mercury. Mercury speciation analyses were conducted using a modified U.S. Environmental Protection Agency (EPA) Method 29 developed by Radian International at the furnace outlet, heat exchanger inlet, and baghouse inlet corresponding to flue gas temperatures of 970°, 620°, and 250°C, respectively. An additional mercury speciation measurement was performed at the baghouse inlet using a modified EPA Method 29 developed by Ontario Hydro Technologies [49]. The mercury emission and speciation measurement capabilities of these modified EPA methods have been demonstrated through dynamic spike tests and method intercomparisons on bench- and pilot-scale flue gas systems [3,50–52]. Chlorine emissions and speciation were measured during the tests using EPA Method 26A and an on-line HCl(g) analyzer (Thermo Environmental Instruments, Model 15C). X-ray diffraction (XRD) analysis of materials was conducted to identify crystalline phases.

3.2. Mercury–oxygen interactions

During the first test, 10 $\mu g/m^3$ of $Hg^0(g)$ was injected into a simple heated (maximum of 1400°C) gas mixture (8.5 mol% O_2, 91.5 mol% N_2). Duplicate mercury speciation measurements at the furnace outlet and heat exchanger inlet, presented in Fig. 3, indicate average $Hg^0(g)$ spike recoveries of 102% and 92%, respectively. The very low concentrations (< 1.7 $\mu g/m^3$) of $Hg^{2+}X(g)$ measured at the furnace outlet and heat exchanger inlet locations (corresponding to flue gas temperatures of 970°C and 620°C, respectively) are probably an artifact of the speciation method, because $Hg^{2+}X(g)$ species are generally unstable at ≥ 620°C. Four mercury speciation analyses at the baghouse inlet indicate that on average 55% of the $Hg^0(g)$ spike was transformed to $Hg^{2+}X(g)$. An additional measurement at the baghouse inlet using another modified EPA Method 29 developed by Ontario Hydro Technologies indicates that 63% of the $Hg^0(g)$ spike was converted to $Hg^{2+}X(g)$. The formation of $Hg^{2+}X(g)$ occurs within a 1.85-m-long, refractory-lined section of the combustor downstream of the 620°C heat exchanger inlet and upstream of the 250°C baghouse inlet sampling locations (Fig. 2). Flue gas residence time in this section is estimated to be < 0.1 s. On-line analyzers indicate that the only gaseous components available to react with $Hg^0(g)$ were 8.5 mol% O_2 and 30 ppmv NO_x. Apparently NO_x was produced from heating the $O_2(g)$–$N_2(g)$ mixture. Kinetic limitations and the short residence time precluded any significant homogeneous $Hg^0(g)$–$O_2(g)$ or $Hg^0(g)$–$NO_2(g)$ reactions to account for the formation of $Hg^{2+}X(g)$ [12,25,36–38]. The formation of $Hg^{2+}X(g)$ must therefore involve a heterogeneous or catalytic reaction on refractory surfaces in the heat exchanger section of the combustor. Possible reaction products in the $Hg^0(g)$–$NO_2(g)$ system include mercury nitrite and nitrate compounds, but they are generally unstable at flue gas

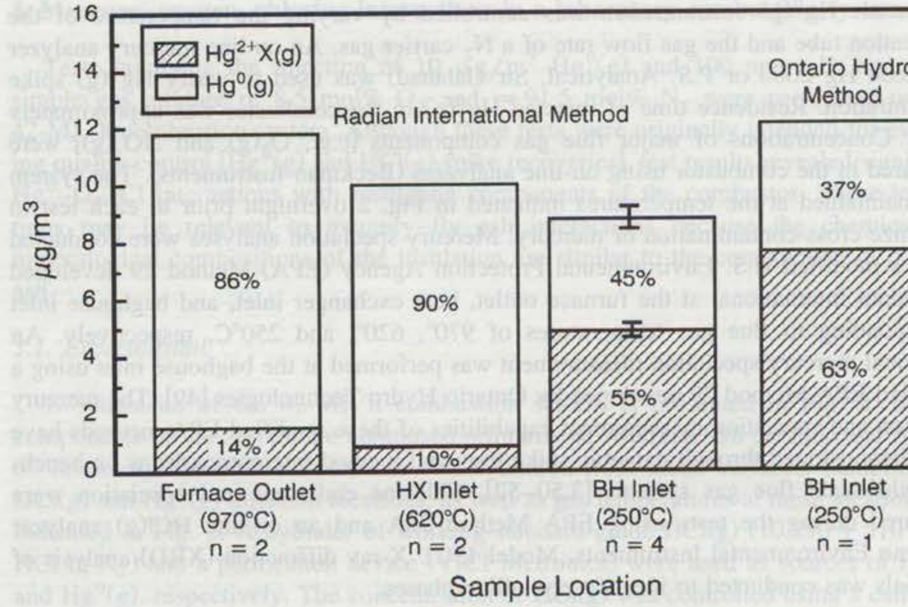

Fig. 3. Mercury speciation results for the 10-µg/m^3 Hg^0(g) baseline spike test. The relative proportions of different mercury species are indicated within each bar as a percent of the total mercury. Error bar represents 95% confidence limits based on four modified (Radian International) EPA Method 29 measurements. Abbreviations: n = number of speciation measurements performed, BH = baghouse, and HX = heat exchanger.

temperatures upstream of the sampling location, > 250°C [19]. Alternatively, the oxidation of Hg^0(g) could involve a heterogeneous reaction with adsorbed (ads) Hg^0 or O$_2$ on surfaces or a catalyzed Hg^0(g)–O$_2$(g) reaction resulting in HgO(g) (decomposes at 500°C) as the reaction product. The most plausible overall reaction is

$$Hg^0(g,ads) + 1/2O_2(g,ads) \xrightarrow{catalyst} HgO(g) \qquad (6)$$

although mercury nitrite or nitrate species could be an intermediate. Chemical and mineralogical (i.e., XRD) analyses indicate that mullite ($Al_6Si_2O_{13}$), dicalcium silicate (Ca_2SiO_4), and the known catalysts corundum (Al_2O_3) and rutile (TiO_2) compose the refractory. Testing by Carey et al. [13] at ≤ 370°C demonstrated that Al_2O_3(s) and TiO_2(s) are Hg^0(g) oxidation catalysts in a simulated coal combustion flue gas. However, in a real coal combustion flue gas, the catalysts are poisoned, possibly because of the presence of fly ash [13].

3.3. Mercury–chlorine interactions

Tests involving the injection of 10 µg/m^3 Hg^0(g) and 100 ppmv HCl(g) into a simple gas mixture of 8.5 mol% O_2(g) and ≈ 91.5 mol% N_2(g) were also performed in the 42-MJ/h combustion system. The purpose of these tests was to determine 100-ppmv

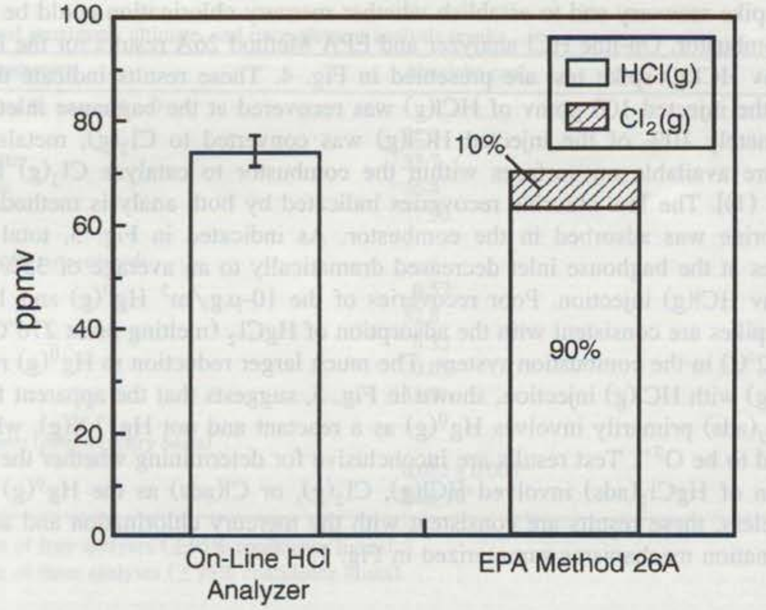

Fig. 4. On-line and EPA Method 26A chlorine analysis results for the 10-μg/m^3 $Hg^0(g)$ + 100-ppmv HCl(g) spike test. Error bar represents 95% confidence limits based on three HCl measurements.

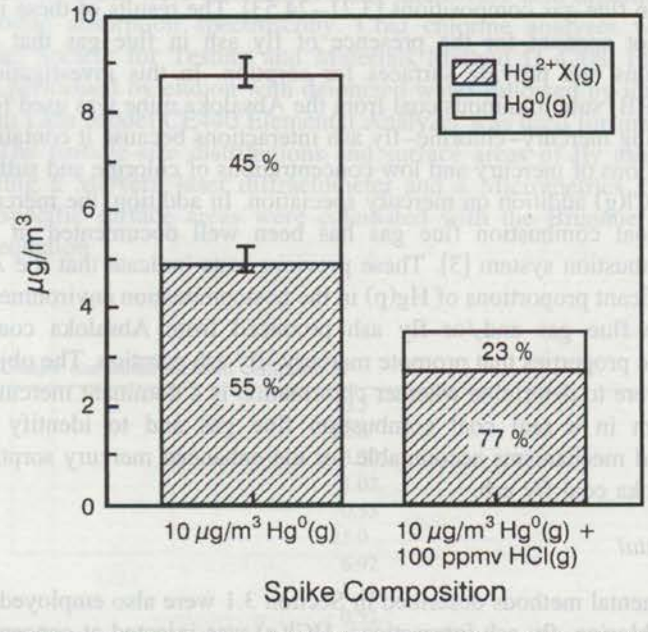

Fig. 5. Mercury speciation results for the 10-μg/m^3 $Hg^0(g)$ baseline spike and 10-μg/m^3 $Hg^0(g)$ + 100-ppmv HCl(g) spike tests. The relative proportions of different mercury species are indicated within each bar as a percent of the total mercury.

HCl(g) spike recovery and to establish whether mercury chlorination could be achieved in the combustor. On-line HCl analyzer and EPA Method 26A results for the $Hg^0(g)$ + 100-ppmv HCl(g) spike test are presented in Fig. 4. These results indicate that about 70% of the injected 100 ppmv of HCl(g) was recovered at the baghouse inlet and that approximately 10% of the injected HCl(g) was converted to $Cl_2(g)$; metals such as Al_2O_3 are available on surfaces within the combustor to catalyze $Cl_2(g)$ formation [reaction (1)]. The low chlorine recoveries indicated by both analysis methods suggest that chlorine was adsorbed in the combustor. As indicated in Fig. 5, total mercury recoveries at the baghouse inlet decreased dramatically to an average of 35% with the 100-ppmv HCl(g) injection. Poor recoveries of the 10-$\mu g/m^3$ $Hg^0(g)$ and 100-ppmv HCl(g) spikes are consistent with the adsorption of $HgCl_2$ (melting point 276°C, boiling point 302°C) in the combustion system. The much larger reduction in $Hg^0(g)$ relative to $Hg^{2+}X(g)$ with HCl(g) injection, shown in Fig. 5, suggests that the apparent formation of $HgCl_2(ads)$ primarily involves $Hg^0(g)$ as a reactant and not $Hg^{2+}X(g)$, where X is suspected to be O^{2-}. Test results are inconclusive for determining whether the apparent formation of $HgCl_2(ads)$ involved HCl(g), $Cl_2(g)$, or Cl(ads) as the $Hg^0(g)$ reactant. Nevertheless, these results are consistent with the mercury chlorination and adsorption transformation mechanisms summarized in Fig. 1.

4. Mercury–chlorine–fly ash interactions in a coal combustion flue gas

Mercury–chlorine interactions have been investigated experimentally using simulated coal combustion flue gas compositions [3,21–24,53]. The results of these investigations, however, do not account for the presence of fly ash in flue gas that may catalyze mercury reactions and provide surfaces for sorption. In this investigation, a Powder River Basin (PRB) subbituminous coal from the Absaloka mine was used for experimentally investigating mercury–chlorine–fly ash interactions because it contains sufficiently high concentrations of mercury and low concentrations of chlorine and sulfur to quantify the effect of HCl(g) addition on mercury speciation. In addition, the mercury speciation of Absaloka coal combustion flue gas has been well documented in tests using a 580-MJ/h combustion system [3]. These previous tests indicate that the Absaloka coal produces significant proportions of Hg(p) in the postcombustion environment (≈ 180°C). Apparently the flue gas and/or fly ash produced from Absaloka coal combustion possess intrinsic properties that promote mercury–fly ash sorption. The objectives of this investigation were to determine whether chlorination is a dominant mercury transformation mechanism in a real coal combustion flue gas and to identify the flue gas components and mechanisms accountable for the enhanced mercury sorption characteristics of Absaloka coal fly ash.

4.1. Experimental

The experimental methods described in Section 3.1 were also employed in investigating mercury–chlorine–fly ash interactions. HCl(g) was injected at concentrations of 50 and 100 ppmv into the combustion region of the 42-MJ/h combustor shown in Fig. 2 while Absaloka coal was being burned. Most of the temperatures in Fig. 2 generally

Table 1
Absaloka coal proximate, ultimate, and trace element analysis results

Analysis parameters	Absaloka coal
Proximate (wt.%, as-received)	
Moisture	22.0
Volatile matter	33.7
Fixed carbon	36.4
Ash	7.90
Ultimate (wt.%, as-received)	
Sulfur	0.57
Carbon	52.8
Hydrogen	6.33
Nitrogen	0.65
Oxygen	31.7
Trace elements (ppm on a dry basis)	
Mercury	0.052 ± 0.005^a
Chlorine	50 ± 10^b

[a] Average of four analyses (±95% confidence limits).
[b] Average of three analyses (±95% confidence limits).

increased by 50°C during the combustion of Absaloka coal. Fly ash was sampled from the baghouse and analyzed for mercury and chlorine after each test. Mercury concentrations in coal and fly ashes were determined using microwave acid digestion followed by cold-vapor atomic absorption spectroscopy. Coal chlorine analyses were conducted using American Society for Testing and Materials Method D 4208. Fly ash chlorine analyses were performed by elution with deionized water followed by ion chromatography. A Leeman Labs Model CE440 Elemental Analyzer was used for measuring carbon in fly ashes. The particle-size distributions and surface areas of fly ash samples were determined using a Malvern laser diffractometer and a Micrometrics Flowsorb 2300, respectively. Specific surface areas were calculated with the Brunauer, Emmett, and Teller (BET) equation.

Table 2
Absaloka coal ash major and minor element composition

SiO_2	36.3
Al_2O_3	22.6
Fe_2O_3	3.30
TiO_2	1.02
P_2O_5	0.53
CaO	25.0
MgO	6.92
Na_2O	1.11
K_2O	0.52
SO_3	1.70
Total	99.0

Table 3
Absaloka coal combustion flue gas compositions

Component	Baseline	50-ppmv HCl spike	100-ppmv HCl spike
Excess O_2 (mol%)	8.48	8.69	8.22
CO_2 (mol%)	10.6	10.7	10.9
CO (ppmv)	390	580	1540
SO_2 (ppmv)	410	380	420
NO_x (ppmv)	960	1110	1030
HCl (ppmv[a])	3	46	105

[a] Calculated value.

4.2. Results

Proximate, ultimate, and major, minor, and trace element analysis results for the sample of Absaloka coal selected for this investigation are presented in Tables 1 and 2. HCl(g) was injected at concentrations of 50 and 100 ppmv into the combustion region of the combustor while Absaloka coal was being burned. Presented in Table 3 are flue gas compositions for the Absaloka coal combustion tests. The flue gas compositions are similar except for a relatively high CO(g) concentration during the 100-ppmv HCl spike test. Chlorine speciation results for the Absaloka combustion tests are presented in Fig. 6. As expected, chlorine was not detected with EPA Method 26A for the baseline test

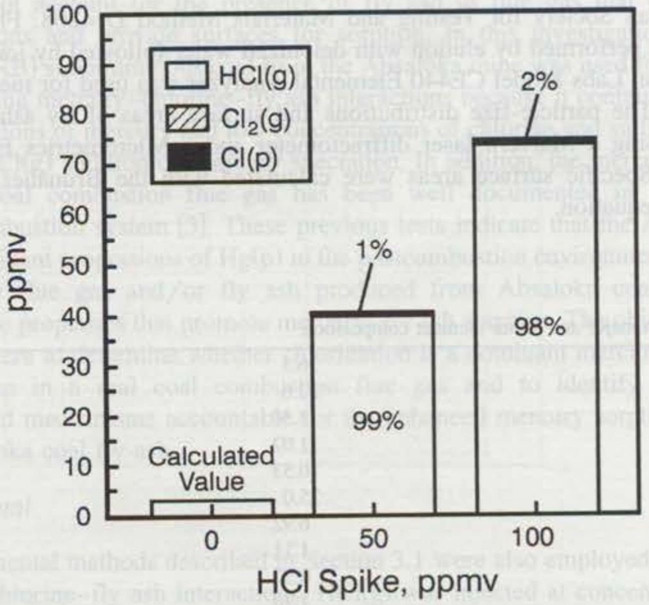

Fig. 6. Chlorine speciation results for the 50- and 100-ppmv HCl(g) injections during Absaloka coal combustion tests.

because of the low chlorine content of Absaloka coal (Table 1). The chlorine speciation result for the baseline test in Fig. 6 is actually a calculated value based on coal chlorine content and assuming 100% HCl(g) speciation. Recoveries of the 50- and 100-ppmv HCl(g) spikes are similar at 82% and 73%, respectively. These HCl(g) recoveries are also similar to those determined for the 10-$\mu g/m^3$ Hg^0(g) + 100-ppmv HCl(g) spike test (refer to Fig. 4). Analogous to the Hg^0(g)–HCl(g) spike test, the relatively low HCl(g) spike recoveries are consistent with the adsorption of chlorine in the combustor. Chlorine speciation results for the 50- and 100-ppmv HCl(g) spikes are very similar. In contrast to the Hg^0(g)–HCl(g) spike testing, however, Cl_2(g) was not detected and particulate chlorine [Cl(p)] composes $\leq 2\%$ of the total chlorine measured.

Mercury speciation results for the Absaloka coal baseline and 100-ppmv HCl(g) injection tests are presented in Table 4 and Fig. 7. Results of the 50-ppmv HCl(g) injection test are not presented because of a lack in repeatability among the three mercury speciation measurements. The mercury mass balance closures in Table 4 provide an indication of data quality and the possibility of mercury retention in the combustor. As shown in Fig. 7, baseline testing of the Absaloka coal indicates that on average 41%, 19%, and 40% of the total mercury in the flue gas was present as Hg(p), $Hg^{2+}X$(g), and Hg^0(g), respectively. In comparison, mercury speciation of the 100-ppmv HCl(g) spiked flue gas was 14% Hg(p), 29% $Hg^{2+}X$(g), and 57% Hg^0(g). Similarly to the Hg^0(g)–HCl(g) spike testing (Fig. 5), total mercury recovery decreased as a result of the 100-ppmv HCl injection. The results in Table 4 indicate that $Hg^{2+}X$(g) and Hg^0(g) concentrations remained constant, within analytical uncertainty, during the baseline and 100-ppmv HCl(g) spike tests, but Hg(p) was significantly depleted as a result of the 100-ppmv HCl(g) injection. The depletion of Hg(p) suggests that the injected HCl(g) reacted with Hg(p), causing mercury adsorption in the combustor, possibly as $HgCl_2$.

Additional evidence for the depletion of Hg(p) as a result of fly ash–HCl(g) interaction is presented in Fig. 8, where baghouse ash chlorine and mercury concentrations are plotted for the three Absaloka coal tests. The results in Fig. 8 indicate that even though the ash scavenged chlorine during the 50- and 100-ppmv HCl(g) injections, the Hg(p) content decreased relative to the baseline Absaloka coal test. A similar plot for ash carbon content is shown in Fig. 9. The significant increase in residual carbon content of the ash produced during the 100-ppmv HCl(g) injection test is reflected by the much higher CO(g) concentration in the flue gas (Table 3). The results in Fig. 9 indicate that

Table 4
Mercury speciation results for absaloka coal tests (mean ± 95% confidence limits)

	Baseline ($\mu g/m^3$)	100-ppmv HCl spike ($\mu g/m^3$)
Hg^0(g)	2.22 ± 0.28	2.40 ± 0.52
$Hg^{2+}X$(g)	1.06 ± 0.05	1.21 ± 0.11
Hg(p)	2.26 ± 0.37	0.60 ± 0.41
Total Hg	5.53 ± 0.65	4.21 ± 0.53
Number of measurements	4	3
Hg mass balance closure	$110 \pm 17\%$	$82 \pm 13\%$

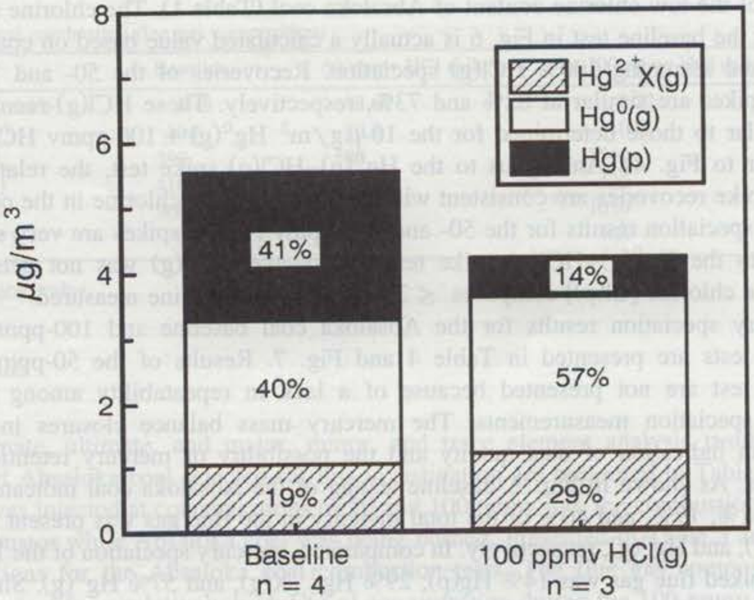

Fig. 7. Average mercury speciation results for the Absaloka baseline and 100-ppmv HCl spike tests. The relative proportions of different mercury species are indicated within each bar as a percent of the total mercury.

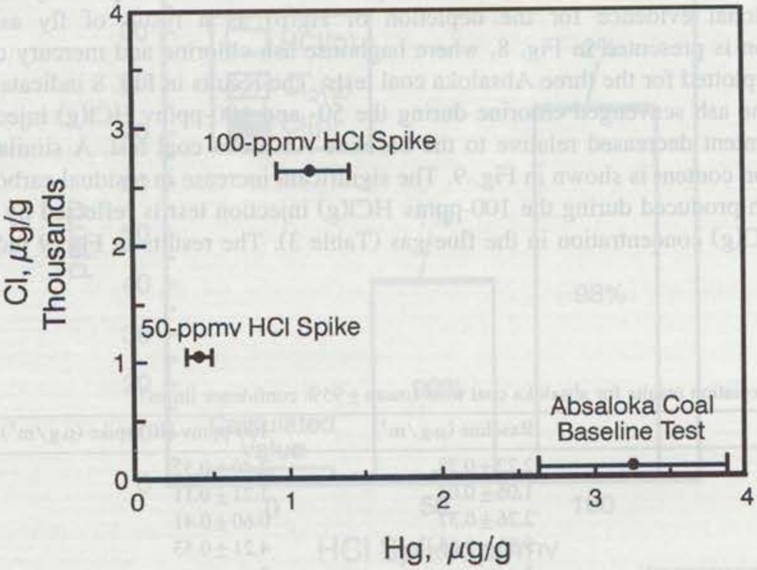

Fig. 8. Chlorine versus mercury concentrations for the Absaloka coal fly ash. Error bars represent 95% confidence limits based on three mercury measurements.

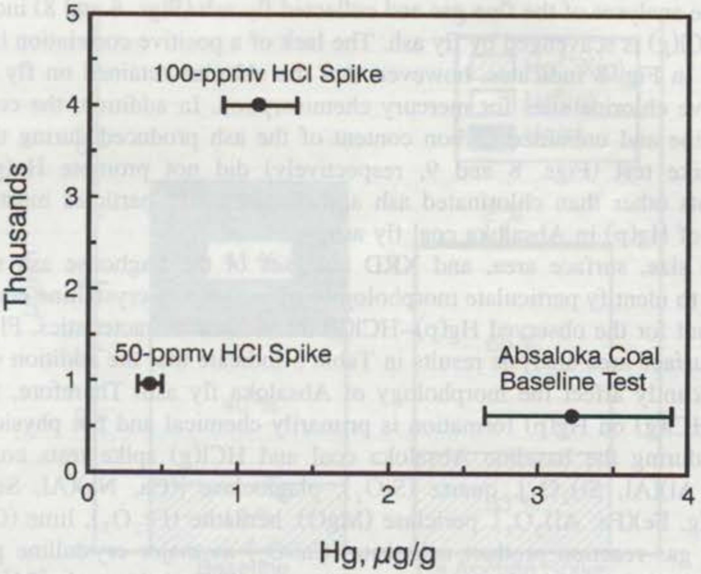

Fig. 9. Carbon versus mercury concentrations for the Absaloka coal fly ash. Error bars represent 95% confidence limits based on three mercury measurements.

an increase in carbon, a potential mercury sorbent, did not correspond to an increase in Hg(p).

4.3. Discussion

Mercury speciation results for the baseline Absaloka coal test, shown in Fig. 7, are very similar to results obtained from burning the pulverized Absaloka coal in a much larger pilot-scale (580-MJ/h) combustion system and measuring mercury speciation using several different methods (Fig. 7–28 in Ref. [3]). Test results from both combustion systems indicate that Absaloka coal combustion flue gas and/or entrained fly ash possess intrinsic properties that promote mercury sorption, as evidenced by relatively high proportions of Hg(p). The similarity in mercury speciation results suggests that the $Hg^0(g)$ oxidation mechanism postulated to occur on refractory surfaces within the 42-MJ/h combustor did not significantly affect the mercury speciation of Absaloka coal combustion flue gas. Apparently the presence of other flue gas components, including ash, impedes reaction (6) from occurring.

A significant depletion in Hg(p) during HCl(g) injection tests, resulting in a relatively low mercury mass balance closure (Table 4), provides indirect evidence for the adsorption of $HgCl_2$ on surfaces within the 42-MJ/h combustor. Based on chlorine mass balance and speciation results (Fig. 6), the apparent formation of $HgCl_2$(ads) involves Cl(ads), HCl(g), or Cl(p) as a reactant. Test results, however, are inconclusive for deciphering the reaction mechanism(s) responsible for the apparent formation of $HgCl_2$(ads).

Chlorine analyses of the flue gas and collected fly ash (Figs. 6 and 8) indicate that the injected HCl(g) is scavenged by fly ash. The lack of a positive correlation between Cl(p) and Hg(p) in Fig. 8 indicates, however, that the chlorine retained on fly ash does not create active chlorine sites for mercury chemisorption. In addition, the combination of high chlorine and unburned carbon content of the ash produced during the 100-ppmv HCl(g) spike test (Figs. 8 and 9, respectively) did not promote Hg(p) formation. Components other than chlorinated ash and carbonaceous particles must promote the formation of Hg(p) in Absaloka coal fly ash.

Particle size, surface area, and XRD analyses of the baghouse ash samples were conducted to identify particulate morphology parameters and crystalline components that may account for the observed Hg(p)–HCl(g) interaction characteristics. Fly ash particle size and surface area analysis results in Table 5 indicate that the addition of HCl(g) did not significantly affect the morphology of Absaloka fly ash. Therefore, the inhibition effect of HCl(g) on Hg(p) formation is primarily chemical and not physical. Fly ashes produced during the baseline Absaloka coal and HCl(g) spike tests contain melilite $[Ca_2(Mg, Al)(Al, Si)_2O_7]$, quartz ($SiO_2$), plagioclase $[(Ca, Na)(Al, Si)_4O_8]$, ferrite spinel $[(Mg, Fe)(Fe, Al)_2O_4]$, periclase (MgO), hematite (Fe_2O_3), lime (CaO), and the CaO–acid gas reaction product anhydrite ($CaSO_4$) as major crystalline phases. Automated scanning electron microscopy analyses by Galbreath et al. [54] indicate that CaO(s) is generally a major component of the fine ash fractions (< 2 μm in diameter) of PRB subbituminous coal fly ashes. CaO(s) and portlandite $[Ca(OH)_2(s)]$, a hydration product of CaO(s), are effective $HgCl_2(g)$ and HCl(g) sorbents [35,55,56]. In bench-scale experiments, Ghorishi and Gullett [35] found that the presence of HCl(g) inhibits the adsorption of $HgCl_2(g)$ by $Ca(OH)_2(s)$. They hypothesized that this inhibition effect was a result of reactive competition between the acidic gases for the available alkaline sites. The inverse relationship between Hg(p) and Cl(p) documented in this investigation is consistent with the hypothesis of Ghorishi and Gullett [35], thus implying that CaO(s) is an important mercury sorption component of Absaloka fly ash.

The hypothesis that CaO(s) is a dominant mercury sorption component of Absaloka fly ash was investigated by adding calcium acetate monohydrate $[Ca(C_2H_3O2)_2 \cdot H_2O]$ to the Absaloka coal to enhance the liberation of organically bound CaO during combustion.The CaO concentration of the Absaloka coal ash increased from 25.0 to 37.6 wt.%, and XRD indicated a significant increase in CaO(s) content as a result of $Ca(C_2H_3O_2)_2 \cdot H_2O$ addition. Mercury speciation measurements in Fig. 10 indicate, however, that the relative proportion of Hg(p) was reduced from 41% of the total mercury in the baseline combustion flue gas to only 2% as a result of CaO(s) addition. Mercury analyses of ashes collected from the baghouse also indicated a reduction from

Table 5
Absaloka fly ash morphological properties

Sample	D_{50} (μm)	BET surface area (m^2/g)
Baseline	5.3	2.67
50-ppmv HCl spike	4.1	2.18
100-ppmv HCl spike	5.7	3.05

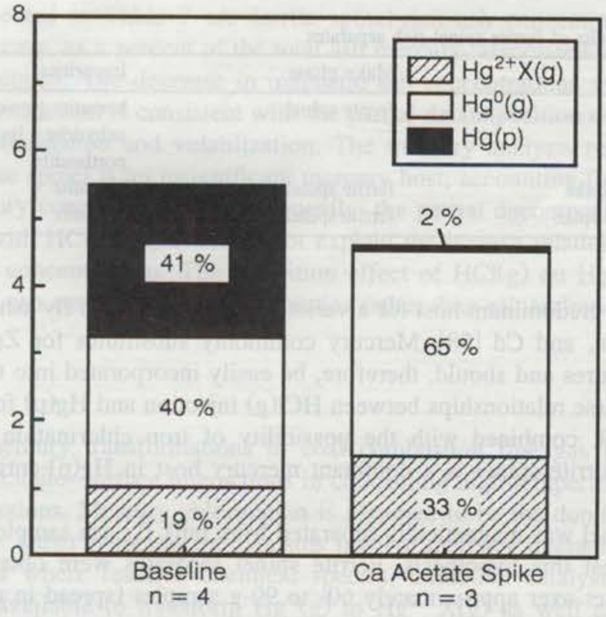

Fig. 10. Average mercury speciation results for the baseline and $Ca(C_2H_3O_2)_2 \cdot H_2O$-spiked Absaloka coal combustion flue gases. The relative proportions of different mercury species are indicated within each bar as a percent of the total mercury.

3.26 ± 1.26 μg/g in the baseline Absaloka fly ash to 0.085 ± 0.044 μg/g in the CaO(s)-spiked ash. Contrary to the hypothesized Hg–CaO(s) adsorption effect, the presence of additional CaO(s) inhibited Hg(p) formation. The added CaO(s) apparently interacted with a gaseous or fly ash component of the flue gas that promotes Hg(p) formation. Alternatively, CaO(s) addition may have affected ash particle morphology.

On-line gas, XRD, particle-size, and surface area analyses indicate that the addition of CaO(s) did not significantly affect the baseline flue gas composition (Table 3), but did affect fly ash mineralogy and morphology. CaO(s) addition promoted the formation of merwinite $[Ca_3Mg(SiO_4)_2]$ at the expense of melilite and plagioclase. The addition of CaO(s) also significantly increased the D_{50} of the baseline Absaloka fly ash from 5.3 to 10.5 μm and decreased BET surface area from 2.67 to 1.60 m^2/g. Based on crystal chemical considerations (e.g., ionic radii, chemical bonding characteristics, cation-site occupancies), the decomposition of melilite and plagioclase cannot account for the inverse relationship between CaO(s) addition and Hg(p) concentration. However, the reduction in particulate surface area and possibly a change in ash surface chemistry are consistent with the decline in Hg(p).

In addition to CaO(s) chlorination, experimental testing by Shimada et al. [57] indicates that iron is readily chlorinated by HCl(g) and then vaporized from coal fly ash. The addition of 50- and 100-ppmv HCl(g) may have resulted in the partial decomposition of ferrite spinel and hematite, the major iron-bearing minerals in the Absaloka fly ashes. In contrast to hematite, ferrite spinel (a thermal decomposition product of pyrite

Table 6
XRD analysis results of ferrite spinel-rich separates

Sample	Major phase	Impurities
Baseline	ferrite spinel	hematite + quartz + anhydrite + lime + portlandite
50-ppmv HCl(g) spike	ferrite spinel	hematite
100-ppmv HCl(g) spike	ferrite spinel	hematite

in coal) is the predominant host for a variety of trace metals in fly ash, including Cu, Cr, Co, Ni, V, Zn, and Cd [58]. Mercury commonly substitutes for Zn and Cd in other mineral structures and should, therefore, be easily incorporated into the spinel structure [59]. The inverse relationships between HCl(g) injection and Hg(p) formation, shown in Figs. 7 and 8, combined with the possibility of iron chlorination and volatilization suggest that ferrite spinel is a dominant mercury host in Hg(p)-enriched Absaloka fly ash.

Ferrite spinel was magnetically separated from bulk fly ash samples and analyzed for mercury to test this hypothesis. Ferrite spinel separates were obtained by passing a canister magnet over approximately 60- to 90-g samples (spread in a thin layer) of the Absaloka baseline and chlorine-enriched ashes. The ashes were agitated numerous times, and the magnetic separation process was repeated until magnetic particles could no longer be collected. Relatively small samples (0.06–0.3 g) of ferrite spinel-rich ash were recovered from the fly ashes using this magnetic separation procedure. XRD analysis results, presented in Table 6, indicate that hematite is a ubiquitous impurity in the ferrite spinel-rich separates. The separate from the baseline Absaloka fly ash also contains quartz, anhydrite, lime, and portlandite as impurities.

Mercury analysis results for the Absaloka bulk fly ash, magnetic ferrite spinel-rich separates, and nonmagnetic ash fractions are presented in Table 7. Mercury analyses of the separates could not be repeated because of the small sample amounts involved. As a quality control measure, a National Institute of Standards and Technology (NIST) Standard Reference Material 1633b subbituminous coal fly ash (0.141 μg/g Hg) was analyzed for mercury in the same manner as the separates. Agreement between the measured and certified mercury values was acceptable, with a relative difference of 11%. The mercury mass balance closures in Table 7 also provide an indication of data

Table 7
Hg analysis results for Absaloka bulk fly ash and magnetic and nonmagnetic fly ash fractions

	Baseline	50-ppmv HCl spike	100-ppmv HCl spike
Bulk ash Hg (μg/g)	3.26 ± 1.26	0.406 ± 0.105	1.16 ± 0.56
Magnetic ash fraction Hg (μg/g)	0.513	0.122	0.627
Magnetic ash fraction (wt.%)	0.35	0.19	0.08
Magnetic ash fraction Hg (%)	0.05	0.06	0.04
Nonmagnetic ash fraction Hg (μg/g)	1.18 ± 0.07	0.438 ± 0.008	1.09 ± 0.04
Hg mass balance closure (%)	36	108	94

quality. Also presented in Table 7 are ferrite spinel-rich ash concentrations and the proportions of mercury, as a percent of the total ash mercury, associated with the ferrite spinel-rich ash fractions. The decrease in magnetic ash concentrations with increasing HCl(g) spike concentrations is consistent with the partial decomposition of ferrite spinel because of iron chlorination and volatilization. The mercury analysis results indicate, however, that ferrite spinel is an insignificant mercury host, accounting for $\leq 0.06\%$ of the total ash mercury concentrations. Consequently, the partial decomposition of ferrite spinel associated with HCl(g) injection cannot explain the inverse relationship between HCl(g) and Hg(p) concentrations. The inhibition effect of HCl(g) on Hg(p) formation probably relates to ash surface chemical properties rather than mineralogical properties.

5. Conclusions

A review of mercury transformations in coal combustion flue gas highlights the importance of particulate–surface interactions in controlling high-temperature Hg^0(g) to $Hg^{2+}X$(s,g) conversions. Mercury chlorination is assumed to be the dominant transformation mechanism. Other potential mechanisms involve mercury interactions with ash particulate surfaces where reactive chemical species, oxidation catalysts, and active sorption sites are available to transform Hg^0(g) to $Hg^{2+}X$(g) as well as Hg^0(g) and $HgCl_2$(g) to Hg(p). The following observations and conclusions from an investigation of Hg^0(g)–O_2(g)–HCl(g) and $Hg^{0,2+}$(g)–HCl(g)–CaO(s)–fly ash interactions in a 42-MJ/h combustor support the proposed mechanisms:

- Approximately 60% of a 10-$\mu g/m^3$ Hg^0(g) spike injected into a simple heated (maximum of 1400°C) gas mixture (8.5 vol% O_2, 30 ppmv NO_x, $\approx$ 91.5 vol% N_2) was transformed rapidly (< 0.1 s) to $Hg^{2+}X$(g) within a 1.85-m-long refractory-lined section of the combustor where gas temperatures decrease from 620°C to 250°C. A Hg^0(g)–O_2(g) reaction catalyzed by Al_2O_3(s) and/or TiO_2(s) components of the refractory is postulated. HgO(g) is the suspected reaction product, although mercury nitrite or nitrate species could be an intermediate.
- On average, 41% of the total mercury (5.5 ± 0.6 $\mu g/m^3$) in a 250°C PRB subbituminous coal combustion flue gas is present as Hg(p). The addition of HCl(g) or CaO(s) into the PRB coal combustion environment, however, inhibits Hg(p) formation in the resulting fly ash. The inhibition effects of HCl(g) and CaO(s) on Hg(p) formation are primarily chemical and physical (i.e., decrease in particulate surface area), respectively.
- Low recoveries of mercury during 100-ppmv HCl(g) injections into a simple gas mixture and PRB coal combustion flue gas suggest that $HgCl_2$ was formed and sorbed onto insulating components of the combustor.

Acknowledgements

We are greatly indebted to Richard Schulz, Carolyn Lillemoen, Kristi Schmalenberg, and Grant Dunham for their sampling and analysis efforts. Although the research described in this article has been funded in part by United States Environmental

Protection Agency (EPA) through Grant No. R 824854-01-0 to the University of North Dakota, it has not been subjected to the Agency's required peer and policy review and therefore does not necessarily reflect the views of the Agency and no official endorsement should be inferred.

References

[1] U.S. Environmental Protection Agency, Mercury Study Report to Congress, Volume I: Executive Summary, Office of Air Quality Planning and Standards and Office of Research and Development, EPA-452/R-97-003, December 1997.

[2] K.C. Galbreath, C.J. Zygarlicke, Mercury speciation in coal combustion and gasification flue gases, Environ. Sci. Technol. 30 (1996) 2421–2426.

[3] D.L. Laudal, K.C. Galbreath, M.K. Heidt, A state-of-the-art review of flue gas mercury speciation methods, Electric Power Research Institute, Palo Alto, CA, November 1996, EPRI Report No. TR-107080.

[4] O. Lindqvist, H. Rodhe, Atmospheric mercury — a review, Tellus 37B (1985) 136–159.

[5] F. Slemr, W.J. Seiler, G. Schuster, Distribution, speciation, and budget of atmospheric mercury, J. Atmos. Chem. 3 (1985) 407–434.

[6] O. Lindqvist, K. Johansson, M. Aastrup, A. Anderson, L. Bringmark, G. Hovsenius, L. Håkanson, Å. Iverfeldt, M. Meili, B. Timm, Mercury in the swedish environment — recent research on causes, consequences, and corrective methods, Water Air Soil Pollut. 55 (1991) 1–261.

[7] B. Hall, The gas phase oxidation of elemental mercury by ozone, Water Air Soil Pollut. 80 (1995) 301–315.

[8] O.W. Hargrove, Jr., J.R. Peterson, D.M. Seeger, R.C. Skarupa, R.E. Moser, Update of EPRI wet FGD pilot-scale mercury emissions control research, EPRI-DOE International Conference on Managing Hazardous and Particulate Air Pollutants, Toronto, Ontario, Canada, August 1995.

[9] W.H. Schroeder, J. Munthe, Atmospheric mercury — an overview, Atmos. Environ. 32 (1998) 809–822.

[10] Y. Otani, C. Kanaoka, C. Usui, S. Matsui, H. Emi, Adsorption of mercury vapor on particles, Environ. Sci. Technol. 20 (1986) 735–738.

[11] P. Schager, B. Hall, O. Lindqvist, Retention of gaseous mercury on fly ashes, Second International Conference on Mercury as a Global Pollutant, Monterey, CA, June 1992.

[12] B. Hall, P. Schager, J. Weesmaa, The homogeneous gas phase reaction of mercury with oxygen, and the corresponding heterogeneous reactions in the presence of activated carbon and fly ash, Chemosphere 30 (1995) 611–627.

[13] T.R. Carey, R.C. Skarupa, O.W. Hargrove Jr., Enhanced control of mercury and other HAPs by innovative modifications to wet FGD processes, Phase I Report for the U.S. Department of Energy, Contract DE-AC22-95PC95260, August 28, 1998.

[14] T. Brown, DOE control technology R&D, Managing Hazardous Air Pollutants Fourth International Conference, Washington, DC, November 12–14, 1997.

[15] D.J. Swaine, Trace Elements in Coal, Butterworths, London, 1990, p. 292.

[16] J.C. Groen, J.R. Craig, The inorganic geochemistry of coal, petroleum, and their gasification/combustion products, Fuel Process. Technol. 40 (1994) 15–48.

[17] R.B. Finkelman, Modes of occurrence of potentially hazardous elements in coal: levels of confidence, Fuel Process. Technol. 39 (1994) 21–34.

[18] V.M. Goldschmidt, Geochemistry, Oxford Univ. Press, Fair Lawn, NJ, 1954.

[19] B.J. Aylett, The chemistry of zinc, cadmium, and mercury, Pergamon Texts in Inorganic Chemistry, Vol. 18, Pergamon, 1975.

[20] R. Meij, The fate of mercury in coal-fired power plants and the influence of wet flue-gas desulphurization, Water Air Soil Pollut. 56 (1991) 21–33.

[21] P. Schager, The behaviour of mercury in flue gases, Statens energiverk, National Energy Administration, Sweden, Report FBT-91-20, 1990, p. 59.

[22] B. Hall, O. Lindqvist, E. Ljungström ercu, Mercury chemistry in simulated flue gases related to waste incineration conditions, Environ. Sci. Technol. 24 (1990) 108–111.
[23] B. Hall, P. Schager, O. Lindqvist, Chemical reactions of mercury in combustion flue gases, Water Air Soil Pollut. 56 (1991) 3–14.
[24] D.L. Laudal, K.C. Galbreath, C.J. Zygarlicke, Experimental investigation of mercury speciation in coal combustion flue gases, Fourth International Conference on Mercury as a Global Pollutant, Hamburg, Germany, August 1996.
[25] A. Fontijn, Reaction kinetics of toxic metals, The Fifth International Congress on Toxic Combustion Byproducts, Management of Risk from Combustion Sources, Program and Abstracts, University of Dayton, Dayton, OH, June 25–27, 1997, p. 86.
[26] D. Shao, W. Pan, Behavior of chlorine and sulfur during coal combustion, in: K.H. Michaelian (Ed.), International Conference on Coal Science, Banff, Alberta, Canada, September 12–17, 1993, Conference Proceedings, Vol. 1, pp. 656–659.
[27] H. Deacon, U.S. Patent 165 802, July 1875; U.S. Patent 85 370, December 1868; U.S. Patent 118 209, August 1871; U.S. Patent 141 333, July 1875.
[28] H.Y. Pan, R.G. Minet, S.W. Benson, T.T. Tsotsis, Process for converting hydrogen chloride to chlorine, Ind. Eng. Chem. Res. 33 (1994) 2996–3003.
[29] R.L. Lindbauer, F. Wurst, T. Prey, Combustion dioxin suppression in municipal solid waste incineration with sulfur additives, Chemosphere 25 (1992) 1409.
[30] K. Raghunathan, B.K. Gullett, Role of sulfur in reducing PCDD and PCDF formation, Eniron. Sci. Technol. 30 (1996) 1827–1834.
[31] C.L. Senior, L.E. Bool III, G.P. Huffman, F.E. Huggins, N. Shah, A.F. Sarofim, I. Olmez, T. Zeng, A fundamental study of mercury partitioning in coal fired power plant flue gas, Air and Waste Management Association's 90th Annual Meeting and Exhibition, Toronto, Ontario, Canada, June 8–13, 1997, Paper 97-WP72B.08.
[32] C.L. Senior, J.R. Morency, G.P. Huffman, F.E. Huggins, N. Shah, T. Peterson, F. Shadman, B. Wu, Interactions between vapor-phase mercury and coal fly ash under simulated utility power plant flue gas conditions, Air and Waste Management Association's 91st Annual Meeting and Exhibition, June 14–18, 1998, Paper 98-RA79B.04.
[33] S.V. Krishnan, B.K. Gullett, W. Jozewicz, Mercury control in municipal waste combustors and coal-fired utilities, Environ. Prog. 16 (1997) 47–53.
[34] S.V. Krishnan, B.K. Gullett, W. Jozewicz, Control of mercury emissions from coal combustors, EPRI-DOE International Conference on Managing Hazardous and Particulate Air Pollutants, Toronto, Ontario, Canada, August 15–17, 1995.
[35] B. Ghorishi, B.K. Gullett, Fixed-bed control of mercury: role of acid gases and a comparison between carbon-based, calcium-based, and coal fly ash sorbents, EPRI-DOE-EPA Combined Utility Air Pollutant Control Symposium, Washington, DC, August 25–29, 1997, EPRI Report TR-108683-V3, p. 15.
[36] B. Hall, P. Schager, E. Ljungström, An experimental study of the rate of reaction between mercury vapour and gaseous nitrogen dioxide, Water Air Soil Pollut. 81 (1995) 121–134.
[37] C.-Y. Wu, E. Arar, P. Biswas, Mercury capture by aerosol transformation in combustion environments, 89th Annual Meeting of the Air and Waste Management Association, Nashville, TN, June 1996, Paper 96-MP2.02.
[38] D. Laudal, T. Brown, B. Nott, P. Chu, Bench-scale studies to determine the effects of flue gas constituents on mercury speciation, Conference on Air Quality: Mercury, Trace Elements, and Particulate Matter, McLean, VA, December 1–4, 1998.
[39] S.J. Miller, E.S. Olson, G.E. Dunham, R.K. Sharma, Preparation methods and test protocol for mercury sorbents, Air and Waste Management Association's 91st Annual Meeting and Exhibition, San Diego, CA, June 14–18, 1998, Paper 98-RA79B.07.
[40] J.D. Singer (Ed.), Combustion fossil power systems, Combustion Engineering, 3rd edn., Windsor, CT, 1981.
[41] K.A. Graham, A.F. Sarofim, Inorganic aerosols and their role in catalyzing sulfuric acid production in furnaces, J. Air Waste Manage. Assoc. 48 (1998) 106–112.
[42] L.L. Zhao, G.T. Rochelle, Mercury absorption in aqueous oxidants catalyzed by mercury(II), Ind. Eng. Chem. Res. 37 (1998) 380–387.

[43] V.I. Shashkov, I.P. Mukhlenov, E.Ya Beñyash, V.I. Ostanina, M.M. Shokarev, F.I. Vershinina, Effect of mercury vapors on the oxidation of sulfur dioxide in a fluidized bed of vanadium catalyst, Khim. Prom-st. (Moscow) 47 (1971) 288–290.

[44] T.R. Zacharewski, E.A. Cherniak, W.H. Schroeder, FTIR investigation of the heterogeneous reaction of HgO(s) with SO_2(g) at ambient temperature, Atmos. Environ. 21 (1987) 2327–2332.

[45] J.A. Korpiel, R.D. Vidic, Effect of sulfur impregnation method on activated carbon uptake of gas-phase mercury, Environ. Sci. Technol. 31 (1997) 2319–2325.

[46] W. Liu, R.D. Vidić, T.D. Brown, Optimization of sulfur impregnation protocol for fixed-bed application of activated carbon-based sorbents for gas-phase mercury removal, Environ. Sci. Technol. 32 (1998) 531–538.

[47] M.I. Guijarro, S. Mendioroz, V. Muñoz, Effect of morphology of sulfurized materials in the retention of mercury from gas streams, Ind. Eng. Chem. Res. 37 (1998) 1088–1094.

[48] W.H. Schroeder, G. Yarwood, H. Niki, Transformation processes involving mercury species in the atmosphere — results from a literature survey, Water Air Soil Pollut. 56 (1991) 653–666.

[49] K.E. Curtis, K.E. Eagleson, Speciation of mercury emissions from Ontario Hydro's coal-fired generating stations, Report No. A-F-95-22-Con, Ontario Hydro Technologies, Toronto, Ontario, Canada, March 1995, p. 30.

[50] D.L. Laudal, M.K. Heidt, B.R. Nott, T.D. Brown, Recommended methods for mercury speciation measurements in coal combustion systems, Managing Hazardous Air Pollutants Fourth International Conference, Washington, DC, November 12–14, 1997.

[51] D.L. Laudal, M.K. Heidt, Evaluation of flue gas mercury speciation methods, Electric Power Research Institute Report No. TR-108988, December 1997.

[52] D. Laudal, B. Nott, T. Brown, R. Roberson, Mercury speciation methods for utility flue gas, Fresenius' J. Anal. Chem. 358 (1997) 397–400.

[53] N.C. Widmer, J.A. Cole, W.R. Seeker, J.A. Gaspar, Practical limitation of mercury speciation in simulated municipal waste incinerator flue gases, The Fifth International Congress on Toxic Combustion By-products, Management of Risk from Combustion Sources, Program and Abstracts, Dayton, OH, June 25–27 1997, p. 66.

[54] K.C. Galbreath, C.J. Zygarlicke, D.P. McCollor, D.L. Toman, Development of a stack-plume opacity index for subbituminous coal-fired utility boilers, in: S.-H. Chiang (Ed.), Proceedings of the 12th Annual International Pittsburgh Coal Conference, Coal — Energy and the Environment, September 11–15 1995, pp. 19–26.

[55] A. Lancia, D. Musmarra, F. Pepe, G. Volpicelli, Adsorption of mercuric chloride vapours from incinerator flue gases on calcium hydroxide particles, Combust. Sci. Technol. 93 (1993) 277–289.

[56] W. Jozewicz, B.K. Gullett, Reaction mechanisms of dry Ca-based sorbents with gaseous HCl, Ind. Eng. Chem. Res. 34 (1995) 607–612.

[57] T. Shimada, T. Kajinami, T. Kumagai, S. Takeda, J. Hayashi, T. Chiba, Characteristics of vaporization of coal ash minerals chlorinated by gaseous hydrogen chloride, Ind. Eng. Chem. Res. 37 (1998) 894–900.

[58] R.J. Lauf, Characterization of the mineralogy and microchemistry of fly ash, Nucl. Chem. Waste Manage. 5 (1985) 231–236.

[59] D. Grdenić, G. Tunell, J.J. Rytuba, in: K.H. Wedepohl (Ed.), Handbook of Geochemistry: Elements La (57) to U (92), chap. 80, Vol. II/5, Springer, Heidelberg, 1978.